ELSEVIER

Journal of Nuclear Materials 290–293 (2001) 346–351

journal of nuclear materials

www.elsevier.nl/locate/jnucmat

Suppression of net erosion in the DIII-D divertor with detached plasmas

W.R. Wampler [a,*], D.G. Whyte [b], C.P.C. Wong [c], W.P. West [c]

[a] *Sandia National Laboratories, MS 1056, P.O. Box 5800, Albuquerque, NM, USA*
[b] *University of California, San Diego, CA, USA*
[c] *General Atomics, San Diego, CA, USA*

Abstract

The ability to withstand disruptions makes carbon-based materials attractive for use as plasma-facing components in divertors. However, such materials suffer high erosion rates during attached plasma operation which, in high power long pulse machines, would give short component lifetimes and high tritium inventories. We present the results from recent experiments in DIII-D, in which the divertor materials evaluation system (DiMES) was used to examine erosion and deposition during short exposures to well-defined plasma conditions. These studies show that during operation with detached plasmas, produced by gas injection, net erosion is suppressed everywhere in the divertor. Net deposition of carbon with deuterium was observed at the inner and outer strike points and in the private flux region between strike points. For these low temperature plasmas ($T_e < 2$ eV), physical sputtering is eliminated. These results show that with detached plasmas, the location of carbon net erosion and the carbon impurity source, probably lies outside the divertor. Physical or chemical sputtering by charge-exchange neutrals or ions in the main plasma chamber is a probable source of carbon under these plasma conditions.

Keywords: D111-D; DiMES; Divertor erosion; Erosion/deposition; Detached plasma

1. Introduction

During attached plasma operation in DIII-D the net rate of erosion of graphite is ~10 nm/s at the outer strike point (OSP) [1]. This erosion is barely noticeable in the present machines, however, in the next generation of higher power longer pulse machines such as ITER, carbon erosion is predicted to be three orders of magnitude higher which imposes major constraints on the design and operation of such machines [2]. Materials and plasma conditions must be chosen to reduce this net erosion. The use of low temperature detached divertor plasmas may provide a way to reduce or eliminate erosion in the divertor.

Detached plasmas have been used in DIII-D to reduce the peak heat flux on the divertor [3,4]. Detached plasmas are produced by injecting gas into the divertor producing a high density low temperature divertor plasma from which power flow to the divertor wall is carried mainly by neutrals and impurity radiation. Due to the low temperature of detached plasmas, the energies of ions and neutrals at the divertor wall are much lower than that for attached plasma operation. With detached plasmas, erosion by physical sputtering is eliminated since the energy of particles incident on material surfaces is below the threshold for physical sputtering. On the other hand, the flux of deuterium to the divertor plate is much higher for detached than for attached plasmas and this could increase chemical erosion of carbon. Carbon also flows from the plasma to the divertor plate, and the net rate of erosion or deposition is the difference between the gross removal and deposition rates. Gross erosion rates can be estimated from the incident deuterium flux and known sputtering yields. However, carbon

* Corresponding author. Tel.: +1-505 844 4114; fax: +1-505 844 7775.
E-mail address: wrwampl@sandia.gov (W.R. Wampler).

0022-3115/01/$ - see front matter
PII: S0022-3115(00)00636-X

deposition from dense low temperature plasmas involves complex plasma and surface chemical processes which are poorly understood and therefore difficult to predict for tokamak conditions. Here we report measurements of the net rate of erosion/deposition for a graphite divertor plate exposed to detached plasmas in DIIID. Two experiments, in which divertor materials evaluation system (DiMES) samples were exposed to detached plasmas at the OSP and in the private flux region, were described in a previous paper [1]. Here we add the results from two new experiments in which DiMES samples were exposed to detached plasmas at a second location near the OSP and at the inner strike point (ISP). These four experiments provide the first measurements of erosion/deposition at a broad range of positions in the divertor during detached plasma operation. The results are compared to similar earlier measurements of erosion by attached plasmas [1].

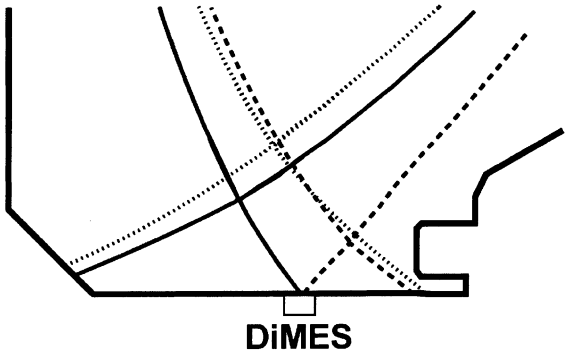

Fig. 1. Schematic of the lower part of DIII-D showing the plasma configuration during the DiMES exposures. The DiMES sample position is indicated by the square. The solid, dashed and dotted lines show the position of the separatrix for exposures to the outer strike point, inner strike point and private flux region, respectively.

2. Sample exposure and analysis

2.1. Experimental methods

The DiMES was used to expose samples to well-defined plasmas for short periods at the DIII-D lower divertor plate and retrieve them for analysis of the resulting erosion or deposition of material [5]. All exposures were done with lower single null divertor plasma configuration. During exposures, the 5 cm diameter samples are flush with the surrounding divertor tiles which are also graphite (Union Carbide ATJ), making the sample part of the divertor floor. The strike point location on the divertor floor is controlled during the discharge to expose the sample only to steady-state divertor plasma conditions. Accumulated exposure times from several similar discharges are typically 10–30 s. Plasma conditions at the DiMES location are determined by radial sweeps of the strike points across Langmuir probes in the divertor floor, and by Thompson scattering, spectroscopy, infrared thermography and other diagnostics. Neutral densities and fluxes in the private flux region are estimated from the measurements of pressure by a capacitance manometer on a port at the DiMES radial location [1].

The mass or number of atoms per unit area (areal density) of the various materials deposited on or eroded from the samples was measured by the MeV ion backscattering for carbon and heavier elements, and nuclear reaction analysis (NRA) for lighter elements ($D(^3He,p)\alpha$ for deuterium, $^9Be(^1H,^4He)^6Li$ for beryllium and $^{11}B(^1H,^4He)^8Be$ for boron) [6–8]. The resolution of the carbon erosion/deposition measurement is about $\pm 1 \times 10^{21}$ atoms/m^2. Conversion of erosion/deposition to units of physical thickness requires the atomic density of the material which is 0.9×10^{29} atoms/m^3 for ATJ graphite, but is likely to be lower for plasma deposited carbon–hydrogen films. Deuterium is incorporated at high concentrations with carbon deposited from deuterium plasmas [9]. Deuterium ions or neutrals can also be energetically implanted, but for the low energies of particles from detached plasmas, the depth of implantation will be a few nanometers or less. Thin metal films were deposited on small regions of some samples to examine metal erosion.

DiMES samples were exposed to detached plasmas at both the outer and inner strike points and in the private flux region between the strike points. The location of the separatrix and the DiMES probe during these exposures is shown schematically in Fig. 1.

2.2. Outer strike point

One sample was exposed twice near the OSP of detached plasmas. During the first exposure, the outer separatrix was centered on the DiMES probe at the major radius $R = 1.48$ m for a total of 13 s. Plasmas were ELMing H-mode confinement regime with 1.4 MA plasma current, 7 MW neutral beam power. D_2 gas was injected into the divertor private flux region increasing the plasma density at the OSP to $n_e \sim 1 \times 10^{20}$ m^{-3} from the normal value of $\sim 4 \times 10^{19}$ m^{-3} in the attached case. The plasma temperature was $T_e \sim 1$–2 eV over the entire OSP region as determined from Thompson scattering, compared to 45–70 eV for attached plasmas. The ion flux at the OSP was broadened with the peak ion flux $\sim 10^{23}$/m^2 s occurring ~ 7 cm outside the separatrix. The incident heat flux from the infrared thermography was also broadened and the peak shifted outside the separatrix compared to attached plasmas. The incident neutral flux was estimated to be $\sim 4 \times 10^{23}$ s^{-1} m^{-2} from the measured divertor pressure of 60 mTorr. This neutral

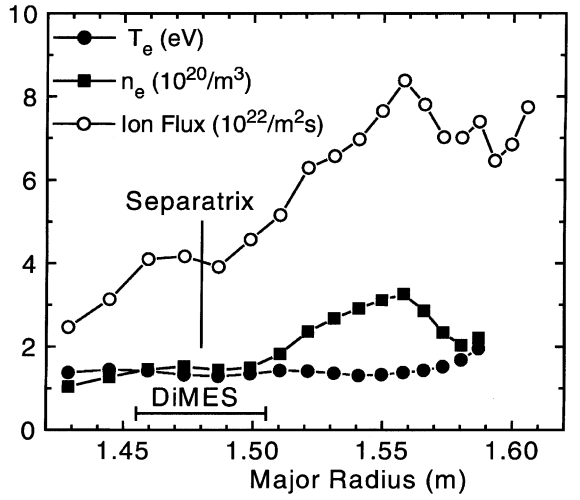

Fig. 2. Detached plasma conditions during exposure at the outer strike point. The horizontal bar shows the location of the DiMES probe during the first exposure. The separatrix was at a major radius of 1.41 m during the second exposure, placing the peak ion flux at the DiMES location.

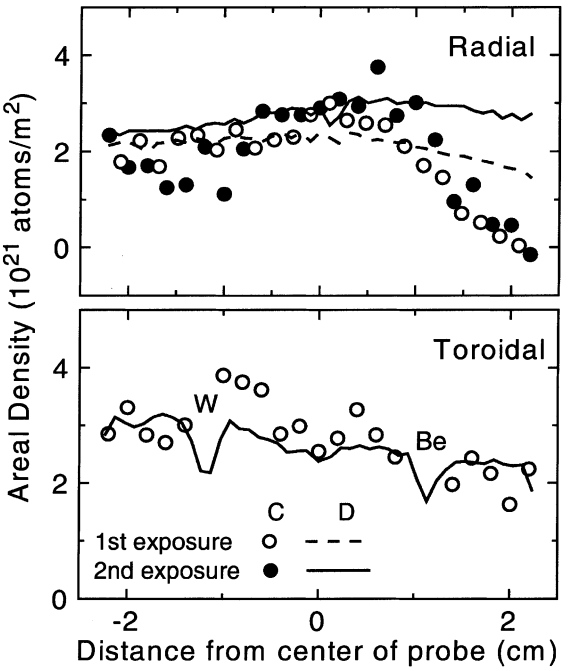

Fig. 3. Measured carbon and deuterium deposition on a DiMES probe exposed to detached plasmas for 13 s at the OSP (first exposure) and just outside the OSP (second exposure). The top panel shows measurements along a line through the center of the probe in the radial direction with increasing major radius from left to right. The bottom panel shows measurements along a line through the center of the probe in the toroidal direction. W and Be indicate the location of tungsten and beryllium films.

flux is an order of magnitude larger than the ion flux. Fig. 2 shows the electron density and temperature and the ion flux, versus major radius for this exposure. Post-exposure ion beam analysis revealed net carbon deposition of $\sim 2 \times 10^{21}$ atoms/m^2, as shown in Fig. 3. Deuterium retention was also $\sim 2 \times 10^{21}$ atoms/m^2. The average net rate of accumulation of carbon and deuterium was therefore $\sim 1.5 \times 10^{20}$ atoms m^2 s^{-1}.

After the first exposure and analysis, the same probe was again exposed to detached plasmas, this time with the separatrix positioned 7 cm inside the DiMES location to place the region of the highest ion flux and heat flux on the DiMES probe. Plasma conditions and exposure time duplicated those of the first exposure. As shown in Fig. 3, the second exposure resulted in no significant additional net erosion or deposition of carbon, and a slight increase in the deuterium retention. From this we conclude that the net carbon deposition rate is lower outside the OSP separatrix, where the ion flux is higher, than at the separatrix. This is consistent with the decreasing carbon deposition outside the separatrix resulting from the first exposure at the OSP shown at the right side of the top panel of Fig. 3.

Erosion of metal was also studied on this sample after the first exposure at the OSP. The sample had films of tungsten and beryllium ~100 nm thick, and 3 mm × 30 mm with the long dimension oriented radially during the exposure. Measurements of the metal film thickness showed that the net erosion of metal was below the detection limit of 2 nm. Ion beam analysis also revealed the presence of carbon covering the metal, consistent with the observation of net deposition of carbon on neighboring carbon surfaces. Metal erosion by sputtering might not be expected under conditions of net carbon deposition, however, in previous experiments similar samples were exposed at the OSP to attached plasmas and erosion of tungsten, mainly by arcing, which was observed in the regions of net carbon deposition. In the present experiments with detached plasmas, the samples showed no evidence of arcing.

2.3. Inner strike point

A sample similar to the one described above, but with tungsten and vanadium metal stripes, was exposed at the ISP of detached plasmas similar to those used for the probe exposures at the OSP described above. The inner separatrix was positioned on the DiMES probe at a major radius of $R = 1.50$ m (see Fig. 1) for a total exposure of 18.2 s. Thompson scattering and Langmuir probe measurements showed that the plasma conditions at the probe (T_e, n_e ion flux) were the same as for the probe exposure at the OSP. The divertor pressure gauge indicated a constant pressure of ~60 mTorr during a

sweep of the ISP across the DiMES location. Hence the neutral flux to the probe at the ISP was also the same as at the OSP.

The resulting net accumulations of carbon and deuterium determined by ion-beam analysis were both in the range from about 2 to 4×10^{21} atoms/m^2 as shown in Fig. 4. The areal density of boron measured by NRA was ~50 times above the detection limit of 10^{18} B/m^2. The ratio of boron to carbon deposition is ~0.02, which is very low considering that most of the carbon in the machine has been covered by a boron film by plasma deposition of diborane [10]. Spectroscopy shows that the B/C ratio in the main plasma is also about 0.02. One way this small B/C ratio could arise is if the carbon comes from small regions with very high erosion rates, such as exposed leading edges, where the boron film is quickly removed, though this mechanism is more likely for attached than for detached plasmas. Alternatively, carbon may come from chemical erosion processes with high selectivity for carbon over boron.

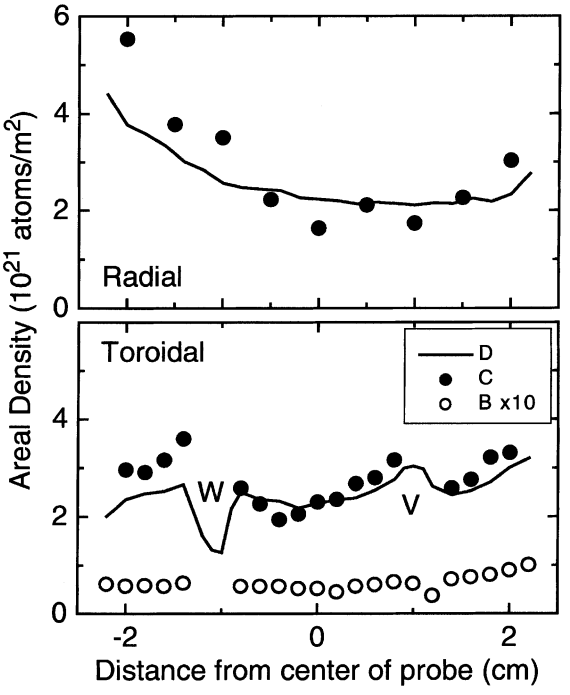

Fig. 4. Measured carbon, deuterium and boron deposition on a DiMES probe exposed for 18.2 s to detached plasmas at the ISP. The top panel shows measurements along a line through the center of the probe in the radial direction with increasing major radius from left to right. The bottom panel shows measurements along a line through the center of the probe in the toroidal direction. W and V indicate the location of tungsten and vanadium metal films.

2.4. Private flux region

The private flux region between the inner and outer strike points receives a high flux of low energy neutral deuterium from molecular dissociation and charge exchange. The flux of neutral deuterium to the private flux region of the divertor, estimated from pressure measurements and D_α emission is an order of magnitude larger than the ion flux estimated from the Thompson scattering measurements. This high flux of atomic deuterium could cause a net chemical erosion of carbon. However, carbon in the plasma can also be deposited onto the private flux region making it a net sink for carbon. To find out if the private flux region is a net source or sink for carbon, a DiMES sample with an implanted Si depth marker but no metal films were exposed for 28 s in the private flux region during a radiative divertor experiment. These plasmas have the OSP placed at the lower cryopump entrance ($R = 1.68$ m) and a large D_2 gas injection (>200 Torr l/s) at the midplane. Argon gas is injected into the divertor through the private flux region resulting in a highly radiative cool dense attached plasma at the OSP. The strong fueling at the midplane and pumping at the OSP produces a flow into the divertor intended to reduce the flow of argon to the main plasma. Carbon remains the primary radiator in the divertor plasma of these discharges [11]. The divertor pressure gauge indicted a pressure of 10–15 mTorr during these discharges. The DiMES sample was located 0.2 m from either strike points and 0.2 m below the X-point. Plasma conditions at the sample determined from Thompson scattering were: $n_e \sim 2.3 \pm 1.4 \times 10^{19}/m^3$, $T_e = 1.5 \pm 0.3$ eV, ion flux 1×10^{22} m^{-2} s^{-1}. Previously reported values [1] of n_e and T_e from Langmuir probe measurements are considered to be less reliable for the cool dense plasma conditions in the PF region. Thompson scattering and Langmuir probes give similar values for n_e near the strike points. The neutral deuterium flux is $\sim 1 \times 10^{23}$ m^{-2} s^{-1}, ~10 times larger than the ion flux. Since the ion energy is below the threshold for physical sputtering, chemical erosion by neutrals should dominate. Analysis of the DiMES sample shows a radially uniform net deposition of carbon and deuterium in the private flux region as shown in Fig. 5.

3. Discussion

During operation with detached plasmas, no net erosion of carbon was found in the DIII-D divertor in contrast to the net erosion previously observed [1] at the OSP of attached plasmas. Net carbon deposition was observed at the rates of 1.5×10^{20} atoms m^{-2} s^{-1} (or 1.7 nm/s assuming the density of graphite) at the OSP, 1.7×10^{20} atoms m^2 s^1 (1.9 nm/s) at the ISP and 0.6×10^{20} atoms m^{-2} s^{-1} (0.7 nm/s) in the private flux

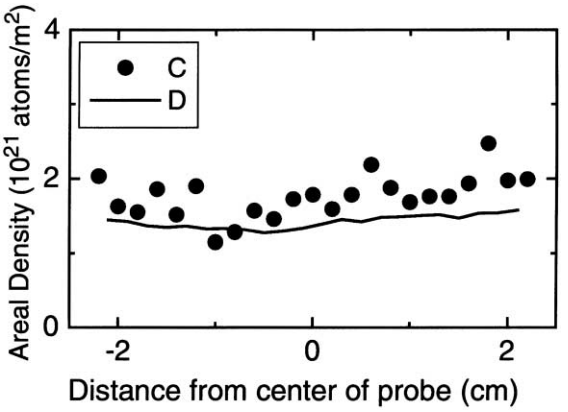

Fig. 5. Measured carbon and deuterium deposition on a DiMES probe exposed for 28 s to detached plasmas in the private flux region along a line through the center of the probe in the radial direction with increasing major radius from left to right.

region. Outside the OSP in the region of peak of ion and heat fluxes, the net carbon erosion/deposition rate was less than 0.5×10^{20} atoms m^2 s^1 (<0.5 nm/s). The observation of carbon deposition in the private flux region, where the ion flux is very low, and the uniform poloidal distribution of carbon deposition, are consistent with carbon deposition mainly as neutrals.

Net deposition in the divertor also indicates that the source of carbon is outside the divertor region. Sputtering from the main chamber wall by neutral deuterium is a likely source of carbon, particularly during fueling by gas injection at the midplane which increases the charge exchange flux at the wall. This source of carbon should be greater for detached than for attached plasmas since the density of neutral deuterium at the edge of the main plasma (and hence the flux of CX neutrals) is about 10 times higher for detached than for attached plasmas, as shown by the measurements at the midplane of pressure and D_α emission. Previous studies in JET also show that the wall of the main chamber undergoes net erosion due to sputtering by charge exchange neutrals, and is a source of impurities [12]. This source of carbon can be reduced either by removing the carbon (e.g. covering it by boronizing, or as in JET by beryllium evaporation) or by reducing the density of neutral deuterium at the main plasma boundary and hence the flux of neutral deuterium to and from the wall. Erosion by ion flux on the inboard wall may also be a source of carbon. This source of carbon would also be greater for detached than for attached plasmas because of the greater width of the scrape-off layer for detached plasmas.

Based on the hydrocarbon molecular spectroscopy, the chemical erosion yield, $Y_{\rm chem}$, at the OSP is measured to be much lower than that expected for detached plasmas in DIII-D. The intensity of CD radical emission at 4308 Å ($B_{\rm CD}$) is an indication of the carbon molecular flux ($\Gamma_{C_xD_y}$) from the plate. The chemical erosion yield for incident ions can be estimated from

$$Y_{\rm chem} = \frac{\Gamma_{C_xD_y}}{\Gamma_{D^+}} = \frac{B_{\rm CD} \cdot (D/XB)_{CD_4}}{\Gamma_{D^+}},$$

where $(D/XB)_{CD_4}$ is the number of CD_4 produced per photon emitted for this transition. Modeling of hydrocarbon transport using WBC and ERO [13,14] calculates $(D/XB)_{CD_4} \sim 6$–10 for detached OSP plasma conditions ($T_e = 1.5$ eV, $n_e = 2 \times 10^{20}$ m^{-3}) of the DiMES exposure. The measured $B_{\rm CD} \sim 0.5$–1×10^{18} ph s^{-1} m^{-2} and incident ion flux $\Gamma \sim 0.5$–1×10^{23} s^{-1} m^{-2} result in $Y_{\rm chem} \sim 10^{-4}$. This value of $Y_{\rm chem}$ is approximately two orders of magnitude lower than the currently recommended values [15,16]. The erosion yield is even smaller if the flux of incident neutral D is included, which is estimated to be an order of magnitude larger than the ion flux. This extremely low $Y_{\rm chem}$ is consistent with the observation of no net erosion in the lower divertor with detached plasmas, where chemical erosion will be the dominant erosion process. The cause of the weak $B_{\rm CD}$, and inferred $Y_{\rm chem}$, is under investigation and is possibly linked to the long-term reduction in DIII-D lower divertor $Y_{\rm chem}$ due to conditioning [10]. The weak $B_{\rm CD}$, and inferred low $Y_{\rm chem}$ could also be due to a probability of prompt local redeposition of hydrocarbon radicals prior to dissociation into CD, which is larger than that assumed in the hydrocarbon transport models, for example due to a change in fragment velocities for dissociation from electronically excited molecular states (Frank–Condon effect).

In measuring the deuterium coverage it was observed that the 700 keV ^{3}He analysis ion beam induced loss of deuterium from the sample as shown in Fig. 6. This ion-

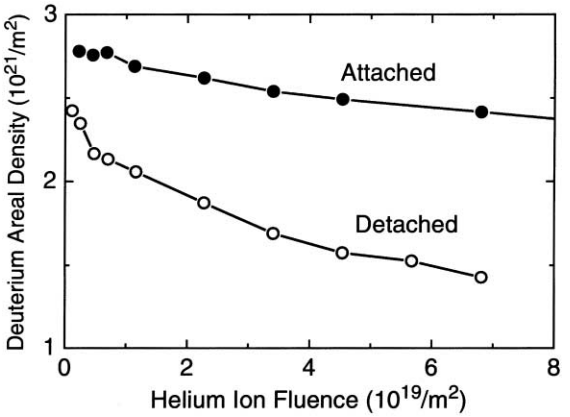

Fig. 6. Areal density of deuterium on DiMES probes exposed at the OSP to attached and detached plasmas versus dose of 700 keV ^{3}He ions.

induced loss of deuterium from carbon is a well-known effect [17] and is the principal mechanism for deuterium removal from tokamaks by helium discharge conditioning. The beam dose normally used for deuterium analysis ($\sim 2 \times 10^{18}$ ions/m^2) was sufficiently small that results shown in Figs. 3–5 are not significantly influenced by this deuterium loss. Ion-induced deuterium release was much faster from samples exposed to detached plasmas than from samples exposed to attached plasmas as shown in Fig. 6. Previous studies show that ion-induced release of deuterium from carbon is faster when the deuterium content of the film is higher [17]. Also it is known that plasma deposition with low incident particle energies (few eV) produces soft low-density polymer-like films with high hydrogen concentration (H/C ratio ~1.2), whereas deposition with higher incident particle energies (>100 eV) produces hard dense films with lower hydrogen content (H/C ~ 0.5) [7]. The faster ion-induced deuterium release from DiMES samples exposed to detached plasmas indicates that these films have high D/C ratio as expected for films deposited by cool dense plasmas. The lower rate of ion-induced release from samples exposed to attached plasmas is consistent with a lower D/C ratio expected for films subjected to bombardment by ions accelerated through the sheath potential of attached plasmas during deposition. Fig. 6 is evidence that the films produced by attached plasmas are of the hard dense type whereas the films deposited by detached plasmas are of the soft polymer-like type. Approximately, half of the deuterium retained in films deposited during detached plasma operation should be released during subsequent operation with attached plasmas. This is likely to impact plasma fueling or machine conditioning.

4. Conclusions

Their ability to withstand disruptions makes carbon-based materials attractive for use as plasma-facing components in divertors. However, the high erosion rates, and resulting short component lifetimes and high tritium inventories, prevent their use in high power long pulse tritium fueled machines for attached plasma operation. Here we have shown that there is no net carbon erosion in the divertor when the divertor plasma is detached. This absence of net erosion allows carbon-based materials to again be considered for use in divertors for detached plasma operation in next-step devices. The net carbon co-deposition in the divertor observed here for detached plasma operation must result from sources of carbon outside the divertor. Elimination of carbon outside the divertor, as in the current ITER design which uses beryllium in the main plasma chamber [18], should reduce the carbon co-deposition in the divertor.

Acknowledgements

This work was supported by the US Department of Energy under contracts DE-AC04-94AL85000 (Sandia National Laboratories) and DE-AC03-98ER54411 (General Atomics).

References

[1] D.G. Whyte et al., J. Nucl. Mater. 266–269 (1999) 67.
[2] G. Federici et al., J. Nucl. Mater. 266–269 (1999) 14.
[3] T.W. Petrie et al., Nucl. Fus. 37 (1997) 321.
[4] C.J. Lasnier et al., J. Nucl. Mater. 266–269 (1999) 577.
[5] C.P.C. Wong et al., J. Nucl. Mater. 258–263 (1998) 433.
[6] J.R. Tesmer, M. Nastasi (Eds.), Handbook of Modern Ion Beam Materials Analysis, Materials Research Society, Pittsburgh, PA, 1995.
[7] W.R. Wampler et al., J. Nucl. Mater. 233–237 (1996) 791.
[8] R. Bastasz et al., J. Nucl. Mater. 220–222 (1995) 310.
[9] W. Jacob, Thin Solid Films 326 (1998) 1.
[10] D.G. Whyte et al., these Proceedings.
[11] M.R. Wade et al., J. Nucl. Mater. 266–269 (1999) 44.
[12] M. Mayer et al., J. Nucl. Mater. 266–269 (1999) 604.
[13] J.N. Brooks, D. Alman, G. Federici, D.N. Ruzic, D.G. Whyte, J. Nucl. Mater. 266–269 (1999) 58.
[14] D. Naujoks, D. Coster, H. Kastelwicz, R. Schneider, J. Nucl. Mater. 266–269 (1999) 360.
[15] B.V. Mech, A.A. Haasz, J.W. Davis, J. Nucl. Mater. 255 (1998) 153.
[16] M. Balden, J. Roth, J. Nucl. Mater. 280 (2000) 39.
[17] W.R. Wampler, S.M. Myers, J. Nucl. Mater. 111&112 (1982) 616.
[18] G. Federici et al., these Proceedings.